Ukrainian Journal of Ecology

Ukrainian Journal of Ecology, 2018, 8(3), 124–139

REVIEW ARTICLE

Evaluation of the usage ratio graphs and energy dissipation in concrete structures with shear walls, under different earthquake records

A. Ahmadi, F. Haghighatbin

Institute of Plant Physiology and Genetics of National Academy of Science of Ukraine, Vasylkivska Str., 31/17, Kyiv, 03022, Ukraine. E-mail: ahmadi90@yahoo.com

Received: 01.05.2018. Accepted: 19.06.2018

Usage Ratio Graphs are used as a tool to assess whether a structure meets performance criteria. As the load factor increases in a gravitational analysis, the relative displacement increases in an Push-Over analysis, or the time increases in a dynamic analysis, the usage graphs show the changes in the usage ratio in accordance with the increment in the load factor, relative displacement or time, respectively depending on the type of the analysis. The responses of a structure under an earthquake can depend on the amount of energy dissipation by the structure. In an analysis of elastic structures, it is generally assumed that energy is dissipated by the viscous damping (this is presented by approximation in modeling, Except for structures that really use viscose dampers). In other hand for the inelastic structures analysis, it is also commonly assumed that in addition with the viscous damping the excess energy is dissipated by inelastic effects (inelastic deformation, failure, etc.). Energy graphs determine which members in the structures have a greater share in inelastic energy dissipation. These graphs help to better estimate the structure's performance. In this study, four "moment frame" concrete structures with irregular planes and moderate ductility and with reinforced concrete shear walls, were analyzed. The Structures are designed in two different shear wall plan configuration, with 8 and 12 stories. The static and dynamic nonlinear analysis of the structures were carried out using the "Perform-3D v5.0" software, which is one of the most powerful tools in the field of nonlinear analysis of structures under earthquake loads.

Keywords: Concrete structures; shear walls; irregular plan; nonlinear dynamic analysis; dissipated energy; usage graph

Introduction

In this study, after performing non-linear dynamic analysis using Perform-3D software, two types of outputs namely energy curves and, usage ratios graphs are analyzed for three levels of performance and two accelerograms pairs. In the next step, the performance levels are introduced and then the energy curves and usage ratios graphs are plotted and the results are analyzed. In Figure 1, the floors plan of the structures and the layout of the shear walls in the structures are shown (Figures 2-26).

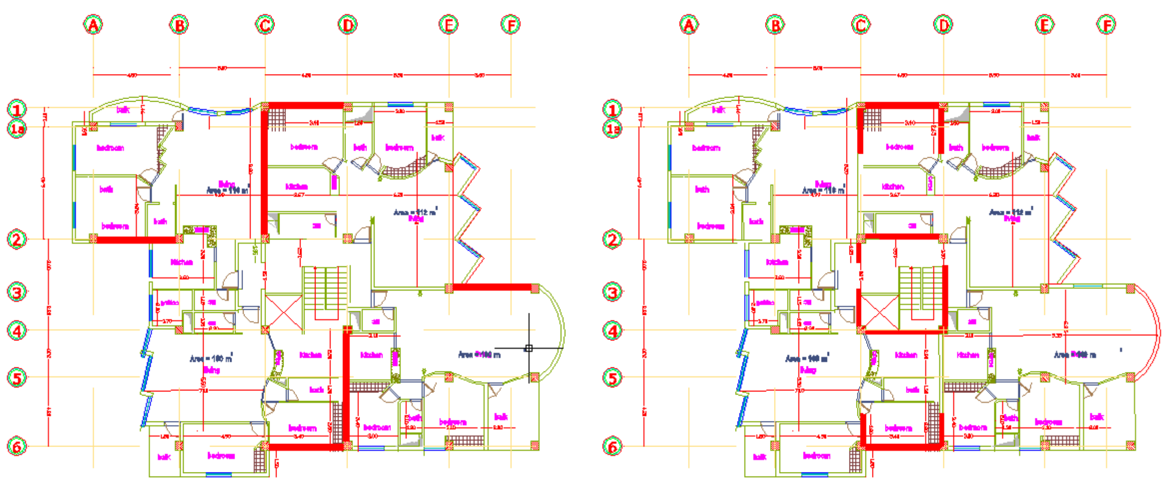

Figure 1. The plan of the subjected structures under and the layouts of shear wall

In Table 1, in this table, S designates the number of classes, SHW1 and SHW2 indicate layout of the "shear wall in the shell" and layout of the "shear wall in the core", respectively.

Table 1. General specification of the subjected frames.

Base shear(ton)	Period of structure(s)	Total height(m)	Fram no.
328/977	0/38	25/4	S8 , SHW1
549/87	0/92	38/2	S12 , SHW1
304/61	0/48	25/4	S8 , SHW2
492/028	1/01	38/2	S12 , SHW2

Performance levels

Performance levels indicate a states of damage that are meet by specific structure and earthquake. The functional levels for the structural and non-structural components are determined individually.

According to the FEMA356 (Federal Emergency Management Agency), there are 5 levels of performance for the structural components, of which 2 levels in the middle and 3 in the main. In this research, damage indicators are compared based on nonlinear static analysis with main performance levels. The three main levels of performance are as follows:

1. The level of IO performance (Immediate Occupancy Level) can be used immediately. At this level, there is no significant damage to the structural components, and these components almost keep all their strength and stiffness after occurrence the earthquake. The non- structural components are safe and keep their performance. The building is suitable for its intended use.
2. Life Safety Level (LS): at this level of performance there are extensive damage and a significant drop in the stiffness of the structural components, but still some margin remains against structural collapse. The non-structural components are safe but use of the building may be impossible before repair.
3. Collapse Prevention Level (CP): at this performance level, major damage to the structural and non-structural components has occurred. The strength and stiffness of the structural components are considerably decreased. There is a risk of the partial collapse.

In this Table 1 we identify the number of classes with the S symbol and the shear wall layout in the shell with SHW1 and the shear wall in the core with the symbol SHW2.

Earthquake selection

In order to study and evaluate the actual behavior of structures against earthquakes, seven pairs of records are selected from the global database of latest recorded earthquake accelerograms. All of the selected earthquakes are far-fault earthquakes and are considered for areas whose distances with a failure fault is at least 25km. The soil type is Sd (375≤vs≤175, vs: shear wave velocity) and are considered in accordance with the Iran's 2800 cod. All of the accelerograms scaled to represent their maximum magnitude. All the seven pairs of the selected earthquake record were scaled in time period from 0.2 T to 1.5 T, in order to have minimum difference with the design spectra from the 2800 code. Table 1 shows the characteristics of the selected records. It should be noted that in this study, only two pairs of accelerograms have been used to obtain the outputs of energy plots and usage ratio graphs (Tables 2-19).

Table 2. Specification of the selected records.

No.	earthquaik	value	Station	Component name	PGA
1	Chi-Chi, Taiwan	MS(7.6)	CHY041	CHY041-N	0.639
				CHY041-W	0.302
2	Kobe	MS(6.9)	Kakogawa	KOBE/KAK000	0.251
				KOBE/KAK090	0.345
3	Kocaeli, Turkey	MS(7.8)	Ambarli	KOCAELI/ATS000	0.249
				KOCAELI/ATS090	0.184
4	Landers	MS(7.4)	Yermo Fire	YER270	0.245
				YER360	0.152
5	Loma Prieta	MS(7.1)	1002 APEEL 2 - Redwood City	LOMAP/A02043	0.274
				LOMAP/A02133	0.22
6	Northridge	MS(6.7)	24303 LA - Hollywood Stor FF	NORTHR/HOL090	0.231
				NORTHR/HOL360	0.358

7	Whittier Narrows	MS(5.7)	90010 Studio City - Coldwater Can	WHITTIER/A-CO2092	0.177
				WHITTIER/A-CO2182	0.231

The usage ratio graphs

The Usage Ratio Graphs are used as a tool to assess whether a structure meets performance criteria. As the load factor increases in a gravitational analysis, the relative displacement increases in an Push-Over analysis, or the time increases in a dynamic analysis, depending on the type of the analysis, the usage graphs show the changes in the usage ratio in accordance with the increment of the load factor, relative displacement, or time respectively.

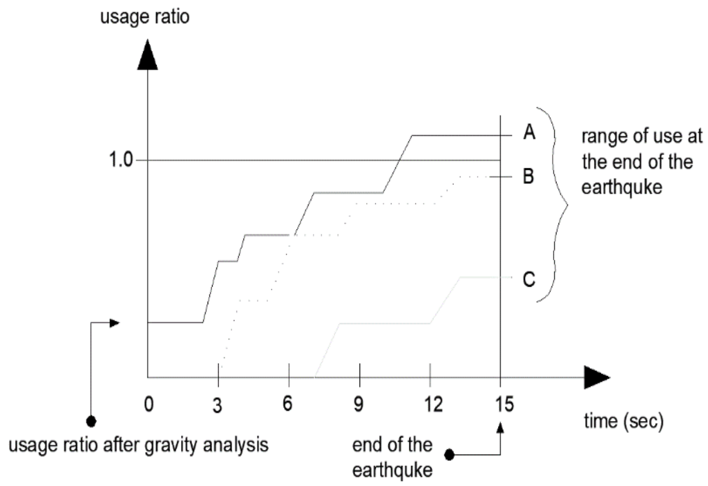

Figure 2. Elements of a usage ratio graph.

In Figure 10, three bound areas are presented. The upper line indicates the maximum usage ratio. As can be seen Considering the three bound areas, obtained from the analysis, the maximum value of the usage ratio for the limit states B and C is smaller than 1, which indicates that the structure meets the performance criteria for these limit states. In other hand this value for limit state A is greater than 1, which indicates that the structures does not meet the performance criteria in this case. It should be noted that, for each structure in this section, only graphs of the usage ratio obtained from the chi chi and Northridge earthquakes are presented.

Usage ratios graphs for 12-story structures with peripheral shear walls

We first examine the 12-story structure with a peripheral shear wall.

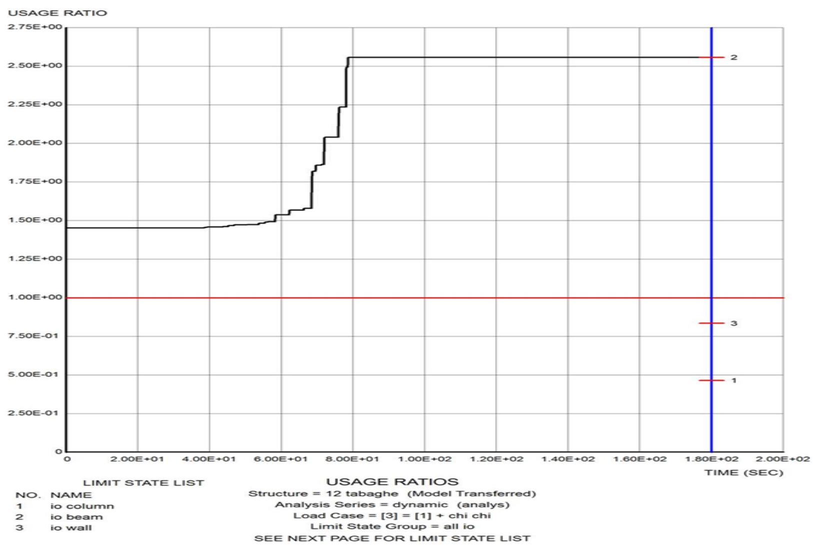

Figure 3. Usage Ratios Graphs of IO hazard level (performance level) for 12-story structures with peripheral shear walls under the chi chi record.

Table 3. The values of the Bound Ratio of IO for all elements of the 12-story structure with a peripheral shear wall under the chi chi record.

wall	beam	column	All Elements
0.8353	2.557	0.4655	Usage Ratios

As can be seen from the figure and corresponding table, under chi chi earthquake, the beams of the structure have exceeded IO hazard level (performance level) and have lost their Immediate Occupancy ability. The columns and shear walls satisfy the performance criteria in this state.

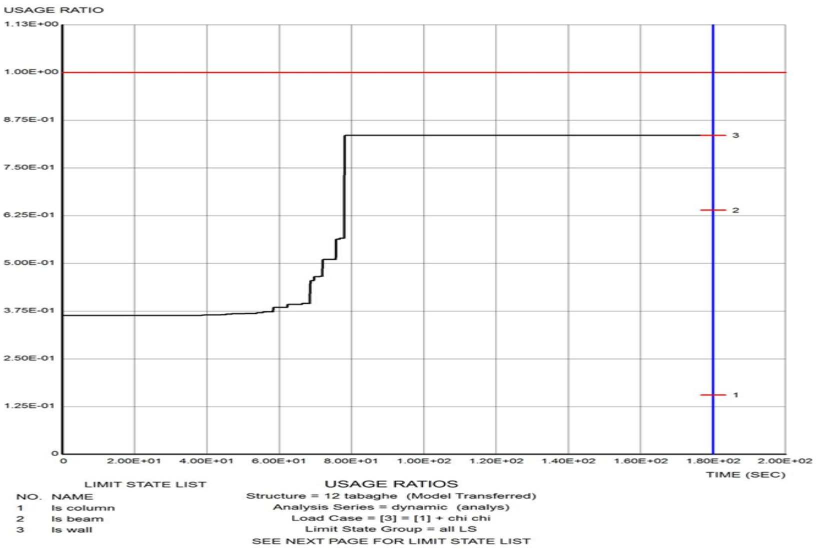

Figure 4. Usage Ratios Graphs of LS hazard level (performance level) for 12-story structures with peripheral shear walls under the chi chi record.

Table 4. The values of the Bound Ratio of LS for all elements of the 12-story structure with a peripheral shear wall under the chi chi record.

Wall	Beam	Column	All elements
0.8353	0.6393	0.1552	Usage Ratios

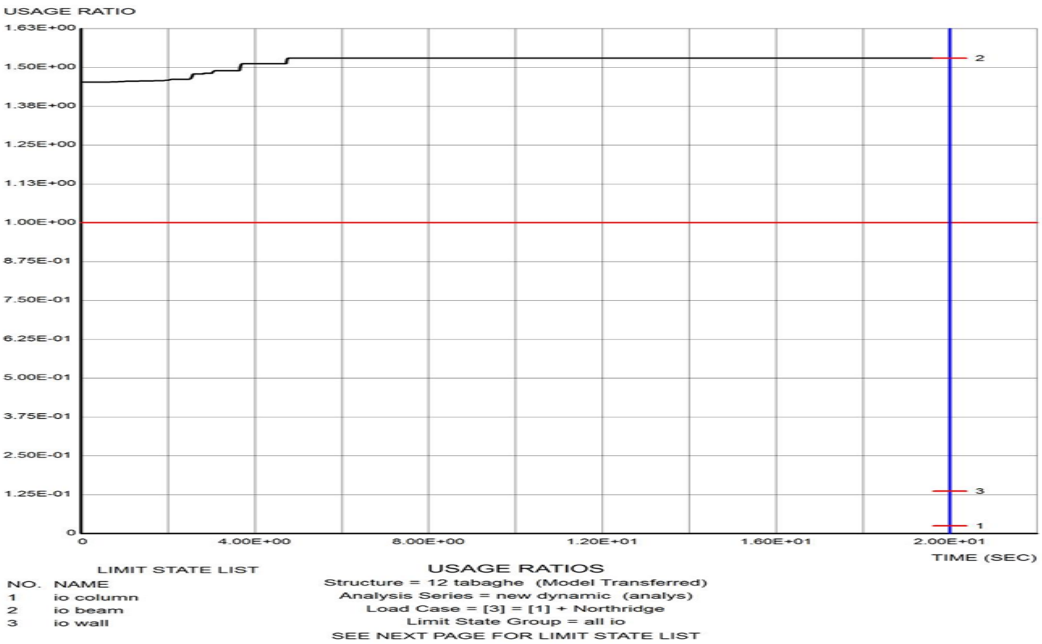

Figure 5. Usage Ratios Graphs of IO hazard level (performance level) for 12-story structures with peripheral shear walls under the Northridge record.

Table 5. The values of the Bound Ratio of IO for all elements of the 12-story structure with a peripheral shear wall under the Northridge record.

Wall	Beam	Column	All Elements
0.1363	1.53	0.02426	**Usage Ratios**

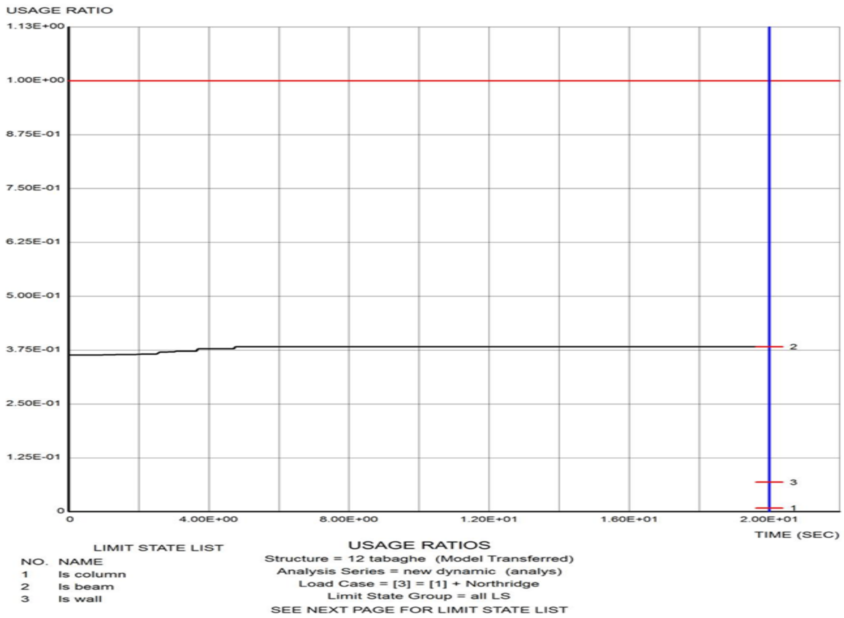

Figure 6. Usage Ratios Graphs of LS hazard level (performance level) for 12-story structures with peripheral shear walls under the Northridge record.

Table 6. The values of the Bound Ratio of LS for all elements of the 12-story structure with peripheral shear wall under the Northridge record.

Wall	beam	column	All Elements
0.06816	0.3825	0.008087	Usage Ratios

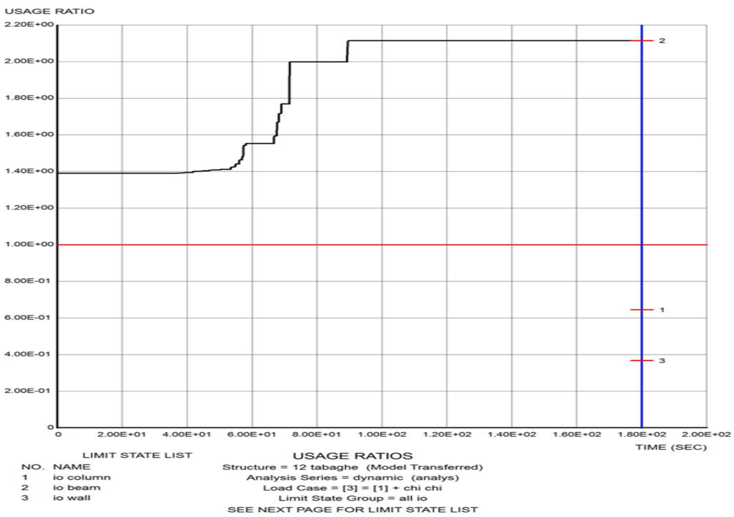

Figure 7. Usage Ratios Graphs of IO hazard level (performance level) for 12-story structures with core shear walls under the chi chi record.

Table 7. The values of the Bound Ratio of IO for all elements of the 12-story structure with core shear wall under the chi chi record.

wall	beam	column	All Elements
0.3678	2.115	0.6452	Usage Ratios

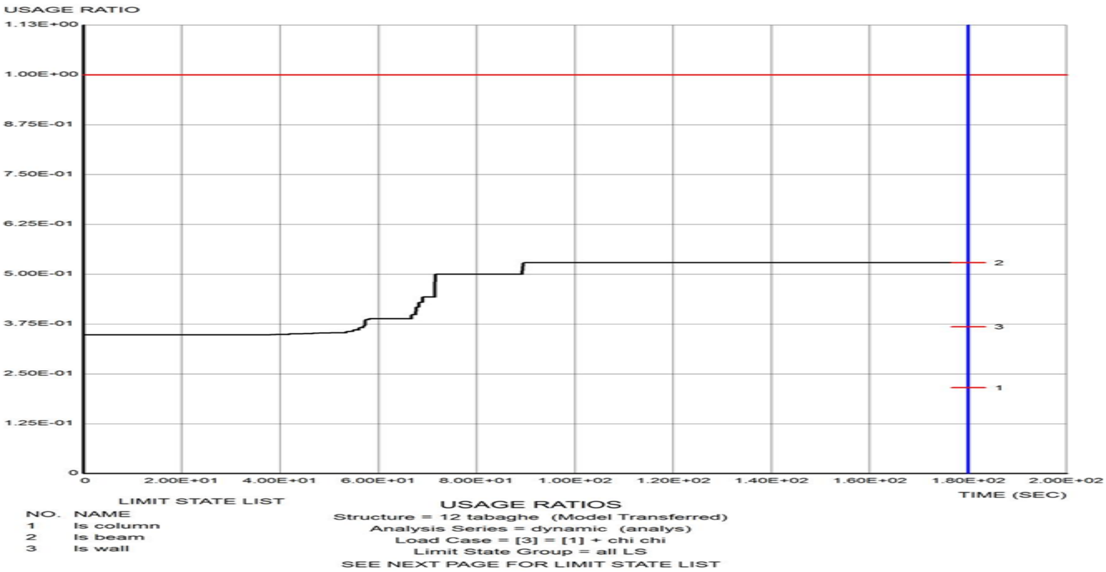

Figure 8. Usage Ratios Graphs of LS hazard level (performance level) for 12-story structures with core shear walls under the chi chi record.

Table 8. The values of the Bound Ratio of LS for all elements of the 12-story structure with core shear wall under the chi chi record.

wall	beam	column	All Elements
0.3678	0.2151	0.5287	Usage Ratios

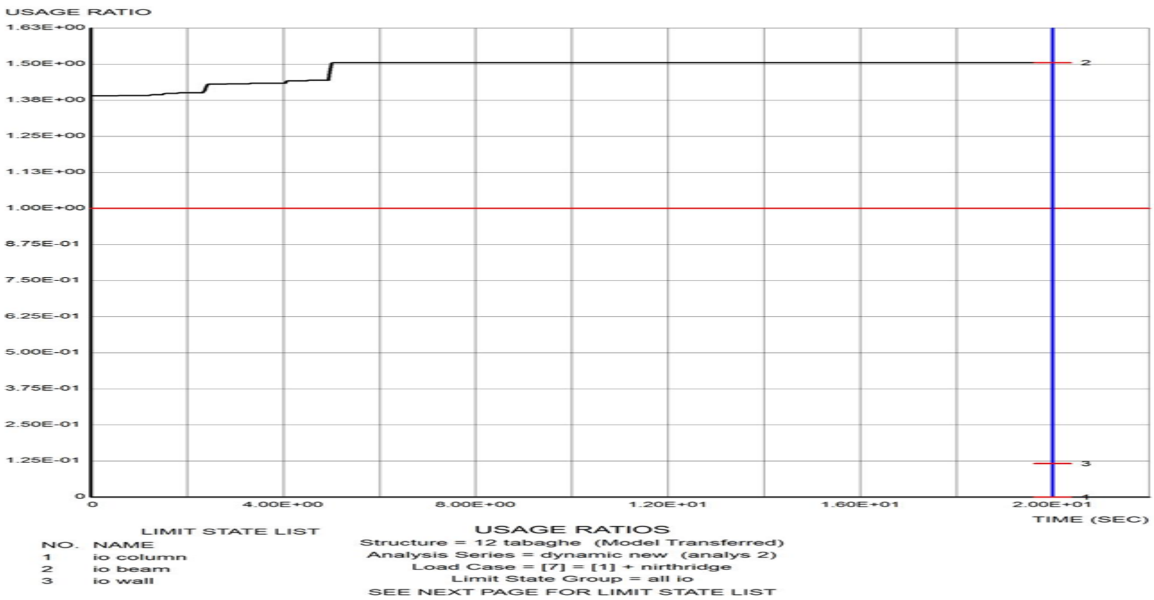

Figure 9. Usage Ratios Graphs of IO hazard level (performance level) for 12-story structures with core shear walls under the Northridge record.

Table 9. The values of the Bound Ratio of IO for all elements of the 12-story structure with core shear wall under the Northridge record.

wall	beam	column	All Elements
0	1.505	0.1163	Usage Ratios

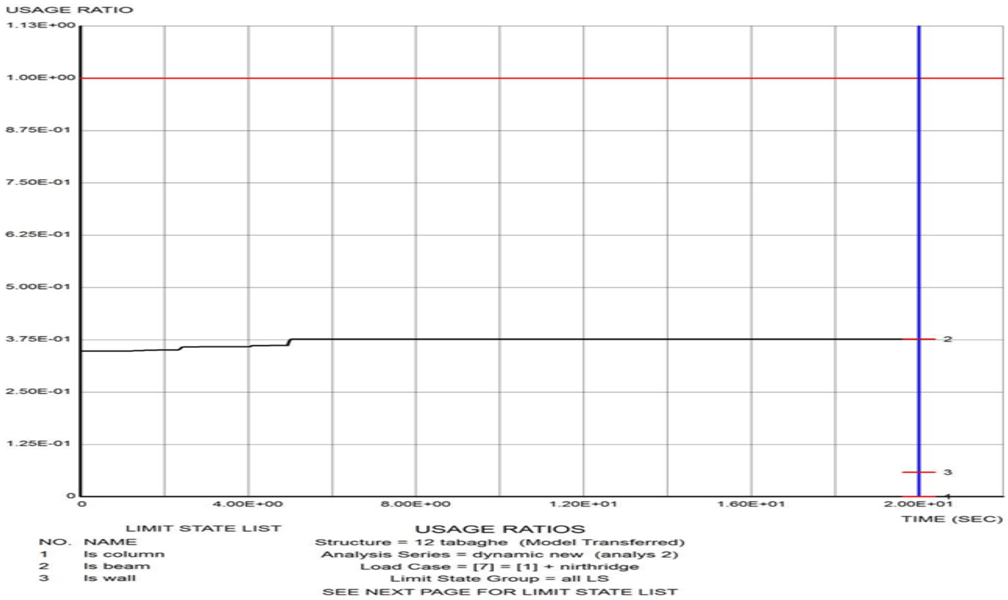

Figure 10. Usage Ratios Graphs of LS hazard level (performance level) for 12-story structures with core shear walls under the Northridge record.

Table 10. The values of the Bound Ratio of LS for all elements of the 12-story structure with core shear wall under the Northridge record.

wall	beam	column	All Elements
0	0.3763	0.05814	Usage Ratios

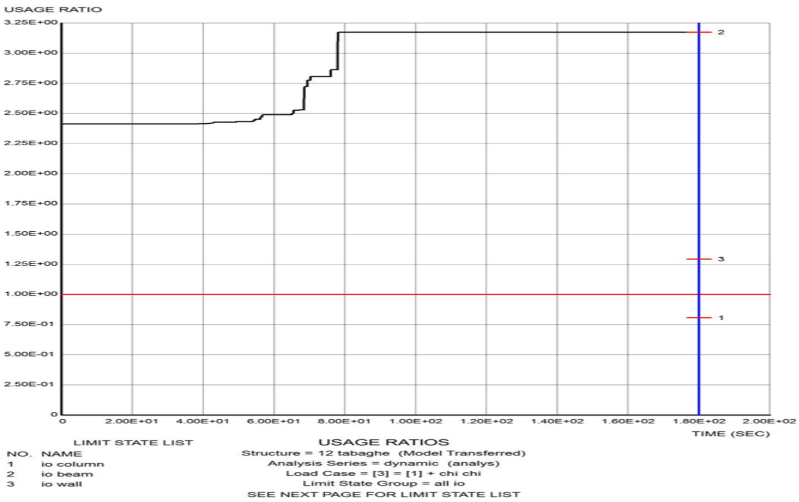

Figure 11. Usage Ratios Graphs of IO hazard level (performance level) for 8-story structures with peripheral shear walls under the chi chi record.

Table 11. The values of the Bound Ratio of IO for all elements of the 8-story structure with peripheral shear wall under the chi chi record.

wall	beam	column	All Elements
0.8069	3.173	1.293	Usage Ratios

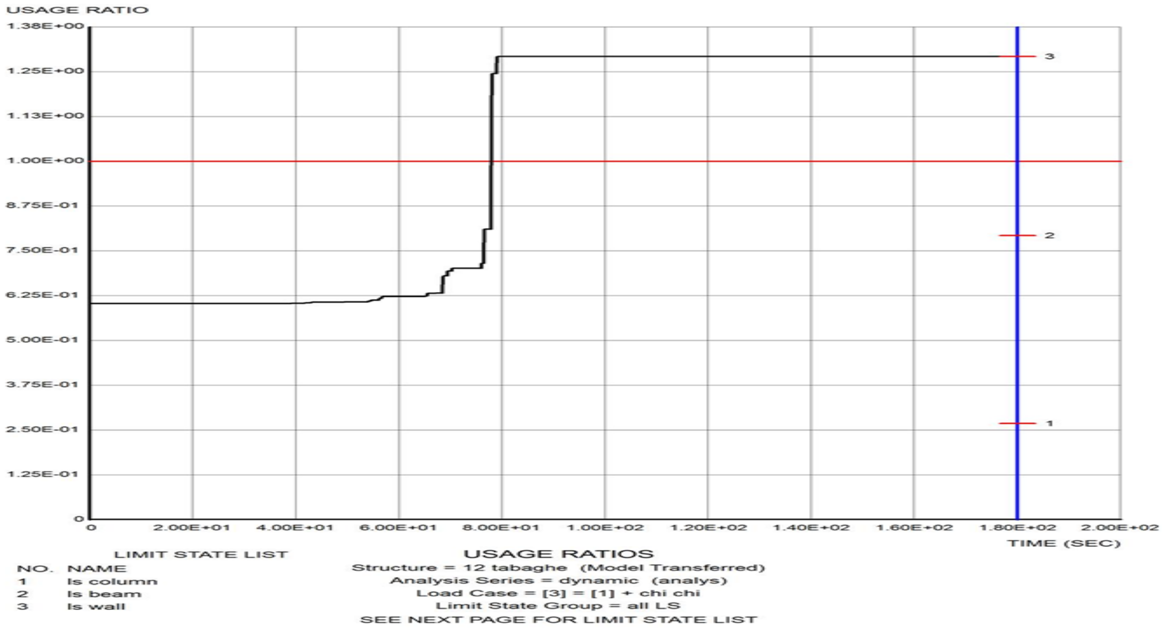

Figure 12. Usage Ratios Graphs of LS hazard level (performance level) for 8-story structures with peripheral shear walls under the chi chi record.

Table 12. The values of the Bound Ratio of LS for all elements of the 8-story structure with peripheral shear wall under the chi chi record.

wall	beam	column	All Elements
0.269	0.7933	1.293	Usage Ratios

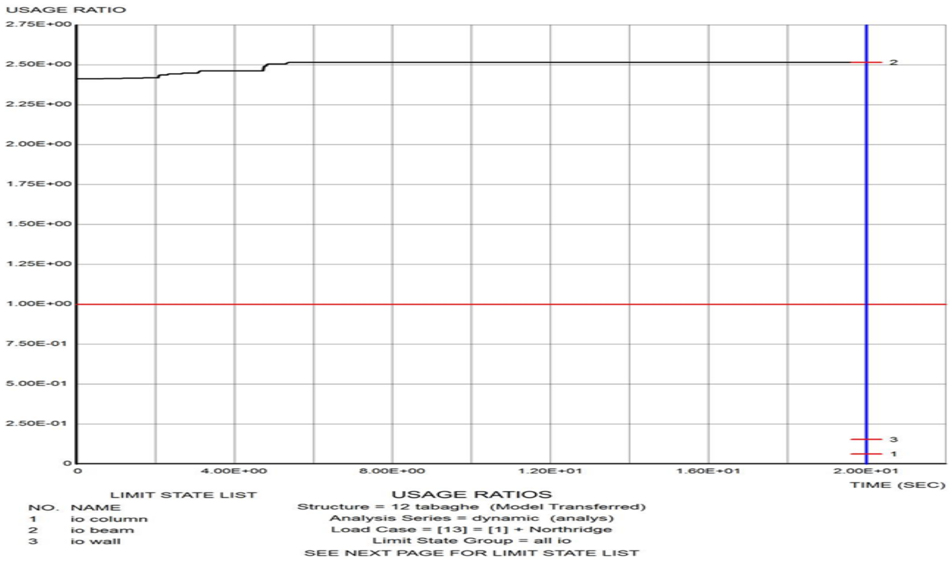

Figure 13. Usage Ratios Graphs of IO hazard level (performance level) for 8-story structures with peripheral shear walls under the Northridge record.

Table 13. The values of the Bound Ratio of IO for all elements of the 8-story structure with peripheral shear wall under the Northridge record.

wall	beam	column	All Elements
0.06258	2.516	0.1539	Usage Ratios

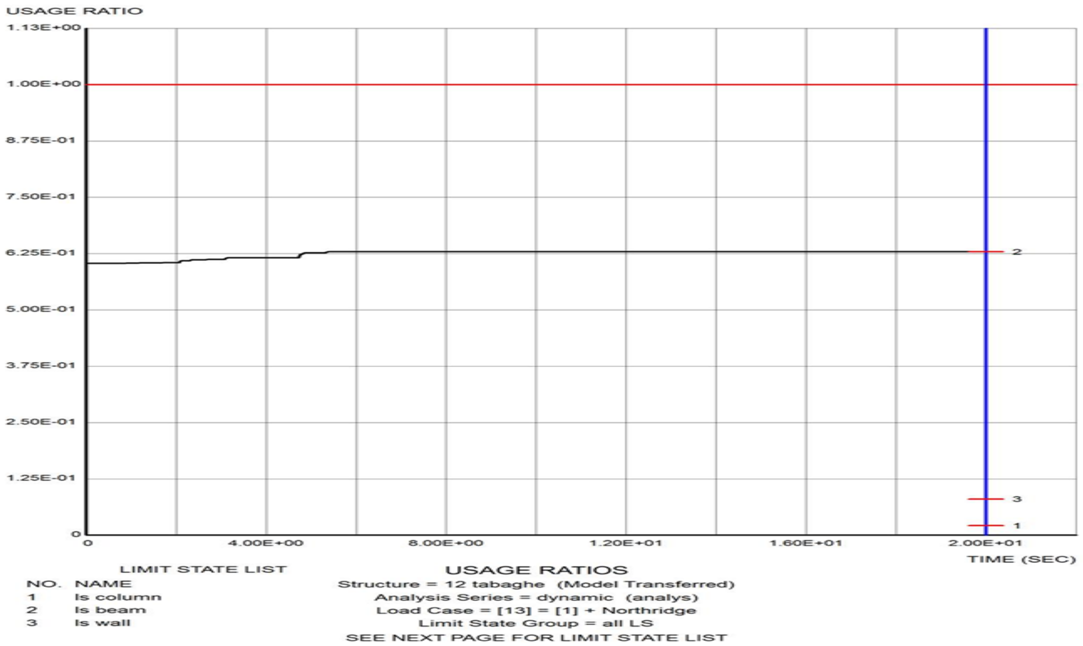

Figure 14. Usage Ratios Graphs of LS hazard level (performance level) for 8-story structures with peripheral shear walls under the Northridge record.

Table 14. The values of the Bound Ratio of LS for all elements of the 8-story structure with peripheral shear wall under the Northridge record.

wall	beam	column	All Elements
0.02086	0.6289	0.07981	Usage Ratios

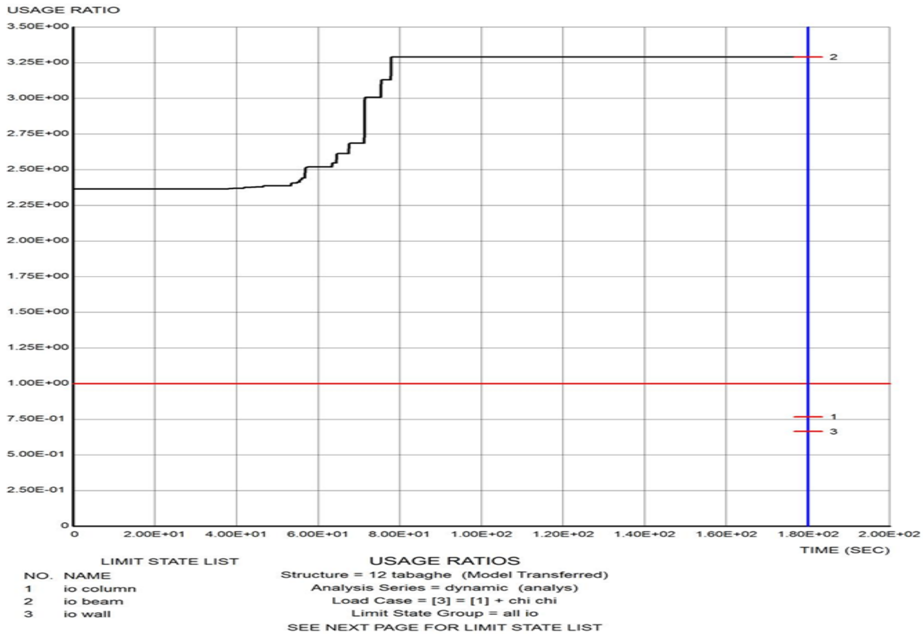

Figure 15. Usage Ratios Graphs of IO hazard level (performance level) for 8-story structures with core shear walls under the chi chi record.

Table 15. The values of the Bound Ratio of IO for all elements of the 8-story structure with core shear wall under the chi chi record.

wall	beam	column	All Elements
0.7673	3.29	0.6642	Usage Ratios

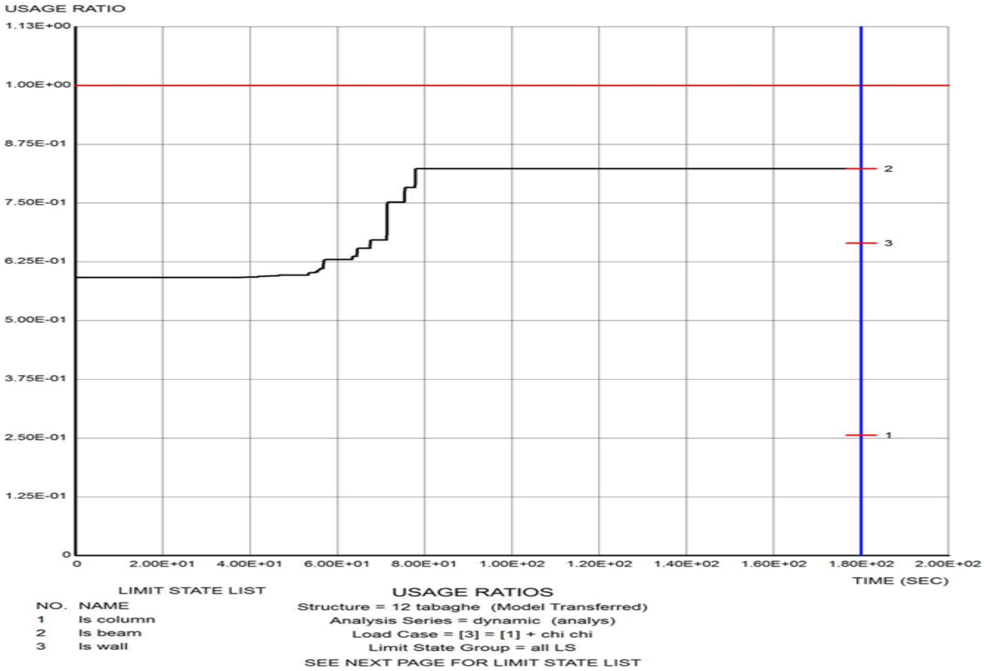

Figure 16. Usage Ratios Graphs of LS hazard level (performance level) for 8-story structures with core shear walls under the chi chi record.

Table 16. The values of the Bound Ratio of LS for all elements of the 8-story structure with core shear wall under the chi chi record.

wall	beam	column	All Elements
0.2558	0.8226	0.6642	Usage Ratios

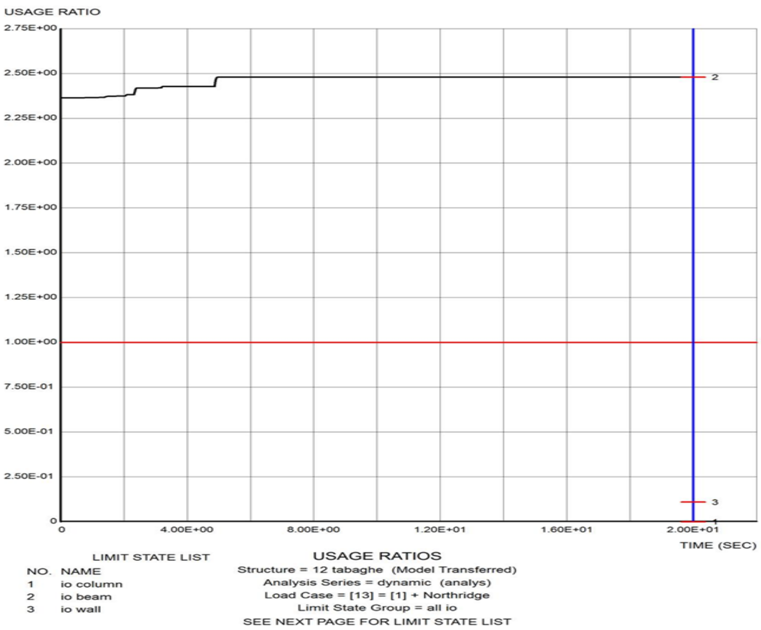

Figure 17. Usage Ratios Graphs of IO hazard level (performance level) for 8-story structures with core shear walls under the Northridge record.

Table 17. The values of the Bound Ratio of IO for all elements of the 8-story structure with core shear wall under the Northridge record.

wall	beam	column	All Elements
0	2.48	0.1091	Usage Ratios

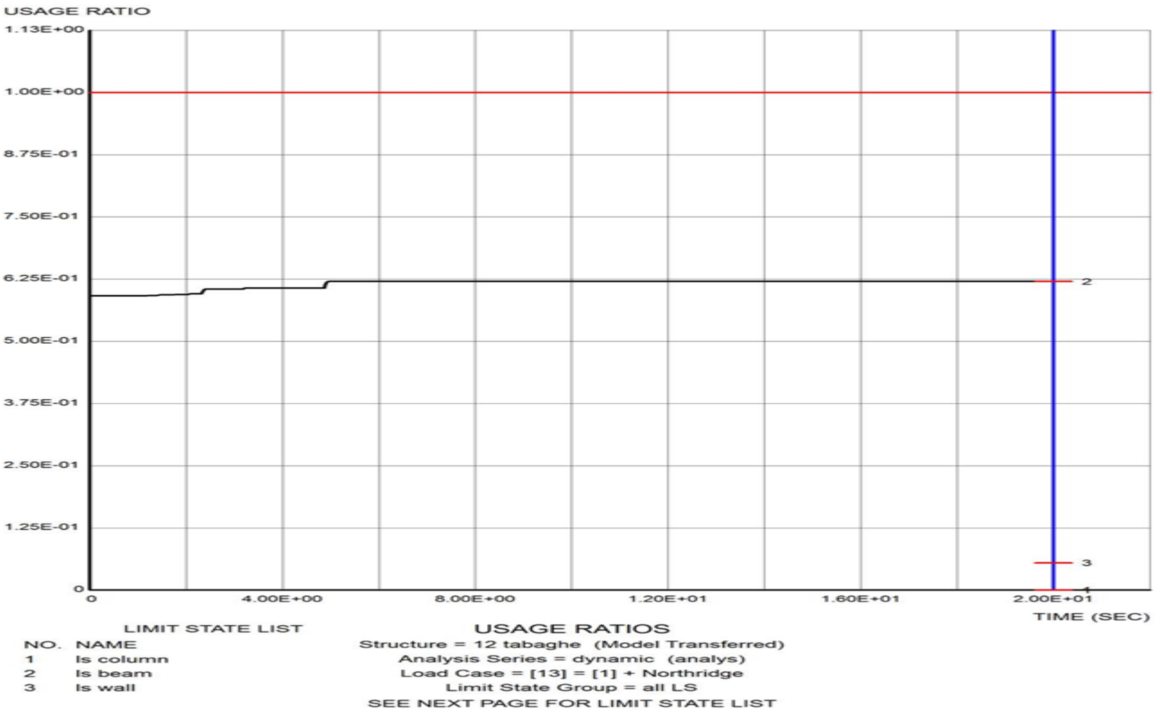

Figure 18. Usage Ratios Graphs of LS hazard level (performance level) for 8-story structures with core shear walls under the Northridge record.

Table 18. The values of the Bound Ratio of LS for all elements of the 8-story structure with core shear wall under the Northridge record.

wall	beam	column	All Elements
0	0.62	0.05456	Usage Ratios

Energy curves

Different form of energy are considered in a dynamic analysis that can be shown as following in the energy plots from the top to bottom, respectively.

1. Kinetic energy of masses. 2-Reversible Strain energy (hardening) of components. 3- Irreversible inelastic energy of components. 4. Viscosity energy dissipated by αM damping. 5. Viscous energy dissipated by βk damping. 6. Viscous energy dissipated by modal damping 7. Viscous energy dissipated by the fluid dampers.

Energy plots from nonlinear dynamics analysis using “Perform 3d” software show the energy input to the structure and the percentage of energy error that in fact can be assumed as the differences between input energy and energy dissipated by the structure. In this section, first, the energy information of each of the structures is summarized in a table, and then we plot the energy graphs for the structures subjected to the selected earthquakes, and finally, the responses of the structures are compared and the obtained results are presented. In this section, for each structures under study, only Chi Chi and Northridge earthquakes energy plots are presented, and energy plots for other accelerograms are given in the appendix.

12-Story structure with peripheral shear wall

First, the energy information of the 12-story structure with peripheral shear wall is summarized in Table 3, and then we plot the energy graphs of this structure Tables 20-22.

Table 19. Summary of energy information for the 12-story structure with peripheral shear wall.

Accelerograms	Energy input to the structure (kgf.m)	Energy error percentage (%)	Dissipated energy
Chi-Chi	1700000	4.09%	69530
kobe	158000	2.39%	3776.2
kocaeli	653800	4.42%	28897.96
Landers	212600	2.15%	4570.9
Loma Prieta	702000	2.37%	16637.4
Northridge	43630	1.56%	680.628
Whittier Narrows	17710	1.21%	214.291

The energy plots of the 12-story structure with peripheral shear wall are as follows.

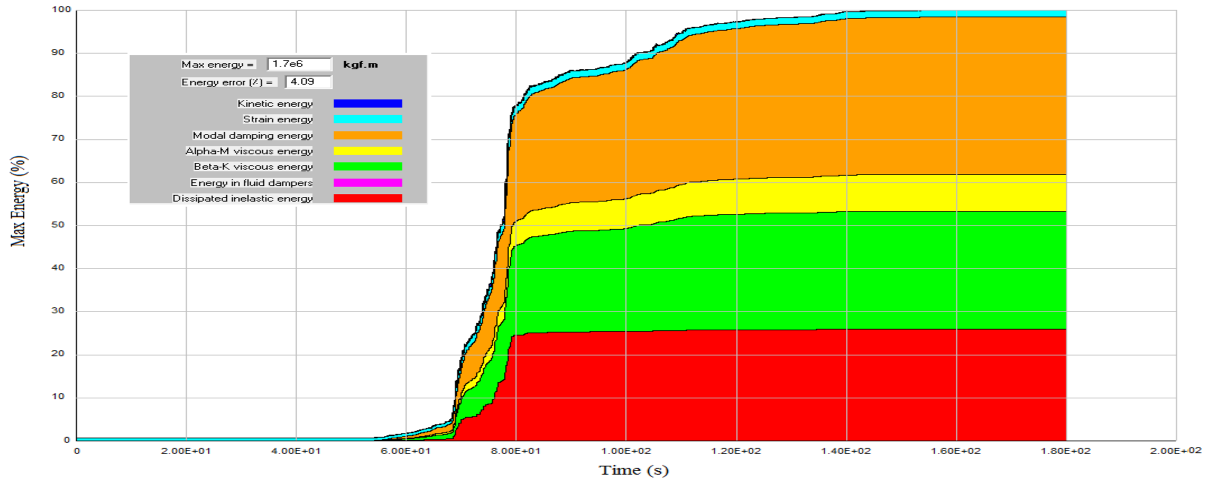

Figure 19. Energy plots for a 12-story structure with peripheral shear wall under the chi chi record.

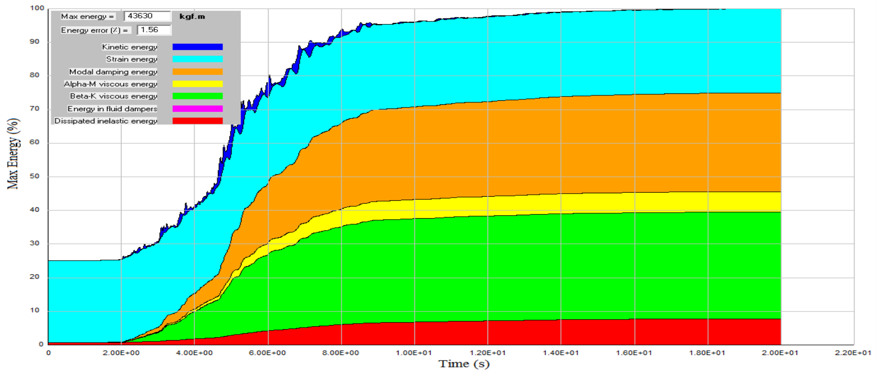

Figure 20. Energy plots for a 12-story structure with peripheral shear wall under the Northridge record.

The energy plots for a 12-story structure with peripheral shear wall under the chi chi record, indicates that after 60 seconds, the structure enters to the nonlinear phase, the minimum amount of the dissipated energy is obtained from the kinetic energy of masses and the maximum amount of the dissipated energy is corresponding to the viscous energy dissipated by βk damping. The amount of energy input to the structure is 1449000 (kgf.m) and the energy error percentage for this earthquake is 5.51. In other hand the energy plots for the 12-story structure with core shear wall under the Northridge record, indicates that after 2 seconds, the structure enters to the nonlinear phase, the minimum amount of the dissipated energy is obtained from the kinetic energy of masses and the maximum amount of the dissipated energy is due the viscous energy dissipated by βk damping. The amount of energy input to the structure is 39770 (kgf.m) and the energy error percentage for this earthquake is 1.81.

12-story structure with core shear wall

For a better comparison with the 12-story structure with peripheral shear wall, the energy information of the 12-story structure with a shear wall in the core is summarized in Tables 4-11, and then we plot the energy graphs for this structure.

Table 20 Summary of energy information for the 12-story structure with core shear wall.

Accelerograms	Energy input to the structure (kgf.m)	Energy error percentage (%)	Dissipated energy
Chi-Chi	1449000	5.51%	79839.9
kobe	128700	3.23%	4157.01
kocaeli	696900	4.61%	32127.09
Landers	161300	2.64%	4258.32
Loma Prieta	577400	2.34%	13511.16
Northridge	39770	1.81%	719.837
Whittier Narrows	15870	1.23%	195.201

The energy plots of the 12-story structure with core shear wall are as follows.

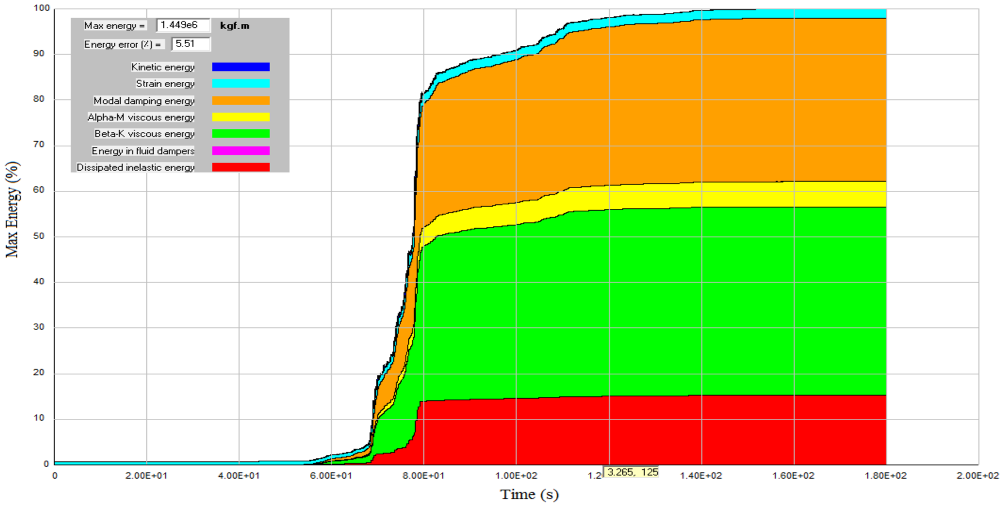

Figure 21. Energy plots for the 12-story structure with core shear wall under the chi chi record.

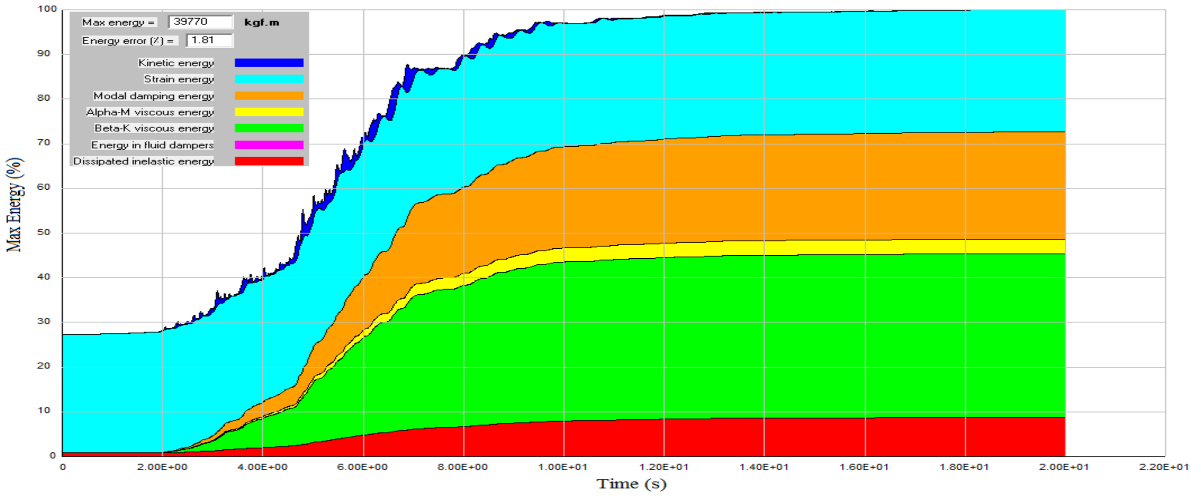

Figure 22. Energy plots for the 12-story structure with core shear wall under the Northridge record.

The energy plots for a 12-story structure with core shear wall under the chi chi record, indicates that after 60 seconds, the structure enters to the nonlinear phase, the minimum amount of the dissipated energy is obtained from the kinetic energy of masses and the maximum amount of the dissipated energy is corresponding to the reversible strain energy (hardening) in the elements. The amount of energy input to the structure is 1700000 (kgf.m) and the energy error percentage for this earthquake is 4.09. In other hand the energy plots for the 12-story structure with the peripheral shear wall under the Northridge record, indicates that after 2 seconds, the structure enters to the nonlinear phase, the minimum amount of the dissipated energy is obtained from the kinetic energy of masses and the maximum amount of the dissipated energy is due to irreversible inelastic energy in the elements. The amount of energy input to the structure is 43630 (kgf.m) and the energy error percentage for this earthquake is 1.56.

8-Story structure with peripheral shear wall

First, the energy information of the 8-story structure with peripheral shear wall is summarized in Table 12, and then we plot the energy graphs of this structure.

Table 21. Summary of energy information for the 8-story structure with peripheral shear wall.

Accelerograms	Energy input to the structure (kgf.m)	Energy error percentage (%)	Dissipated energy
Chi-Chi	1006000	2.70%	27162
kobe	92300	1.46%	1347.58
kocaeli	91090	2.96%	2696.264
Landers	71210	1.65%	1174.965
Loma Prieta	49760	1.42%	706.592
Northridge	49100	0.80%	392.309
Whittier Narrows	17130	0.63%	107.4051

The energy plots of the 8-story structure with peripheral shear wall are as follows.

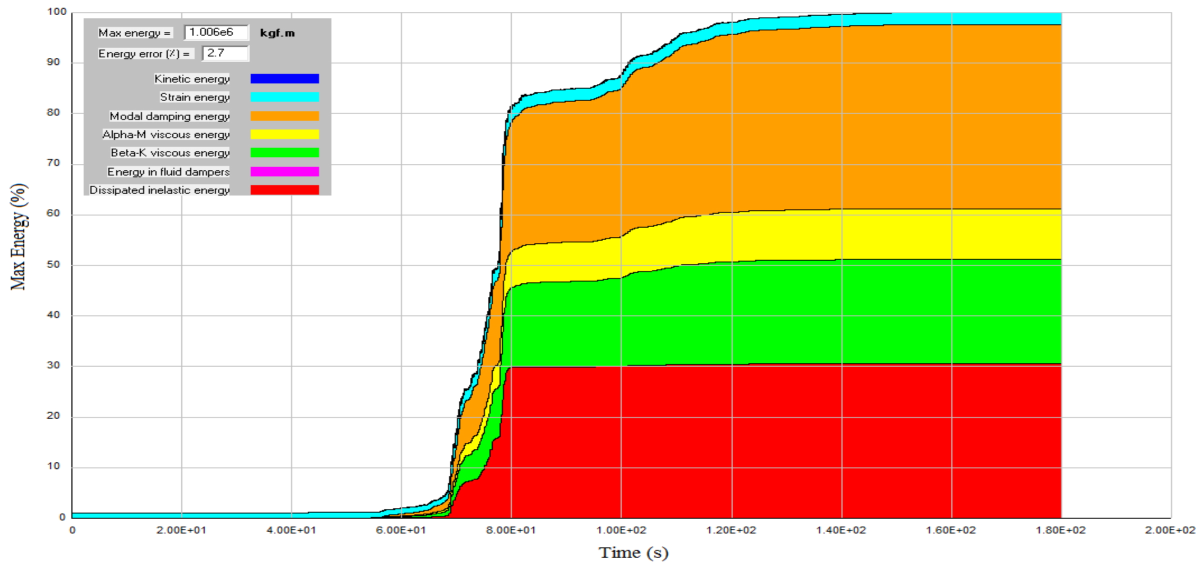

Figure 23. Energy plots for the 8-story structure with peripheral shear wall under the chi chi record.

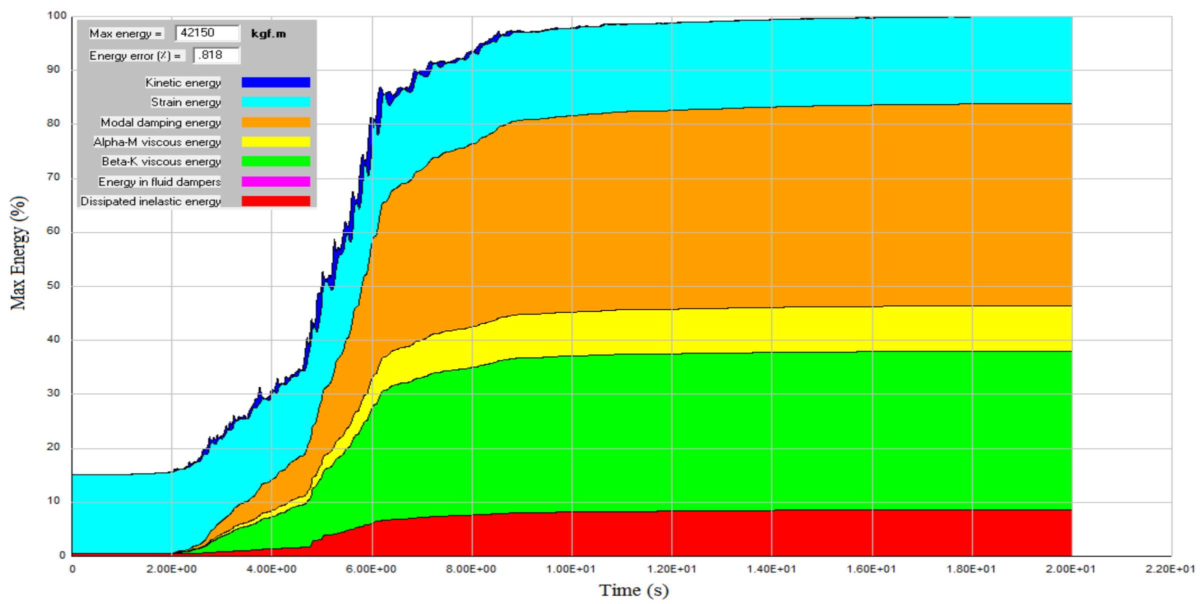

Figure 24. Energy plots for the 8-story structure with peripheral shear wall under the Northridge record.

The energy plots for a 8-story structure with peripheral shear wall under the chi chi record, indicates that after 60 seconds, the structure enters to the nonlinear phase, the minimum amount of the dissipated energy is obtained from the kinetic energy of masses and the maximum amount of the dissipated energy is corresponding to the irreversible elastic in the elements and dissipated energy in fluid dampers. The amount of energy input to the structure is 1006000 (kgf.m) and the energy error percentage for this earthquake is 2.07. In other hand the energy plots for the 8-story structure with the peripheral shear wall under the Northridge record, indicates that after 2 seconds, the structure enters to the nonlinear phase, the minimum amount of the dissipated energy is obtained from the kinetic energy of masses and the maximum amount of the dissipated energy is due to irreversible inelastic energy in the elements and viscose energy by βk dissipating. The amount of energy input to the structure is 42150 (kgf.m) and the energy error percentage for this earthquake is 0.818.

8-Story structure with core shear wall

For a better comparison with the 8-story structure with peripheral shear wall, the energy information of the 8-story structure with core shear wall is summarized in Table 7, and then we plot the energy graphs for the structure.

Table 22. Summary of energy information for the 8-story structure with core shear wall

Accelerograms	Energy input to the structure (kgf.m)	Energy error percentage (%)	Dissipated energy
Chi-Chi	823100	3.89%	32018.59
Kobe	118200	1.96%	2316.72
Kocaeli	331000	2.92%	9665.2

Landers	81160	1.75%	1420.3
Loma Prieta	293600	1.12%	3288.32
Northridge	28130	1.39%	391.007
Whittier Narrows	15870	0.88%	139.656

The energy plots of the 8-story structure with core shear wall are as follows.

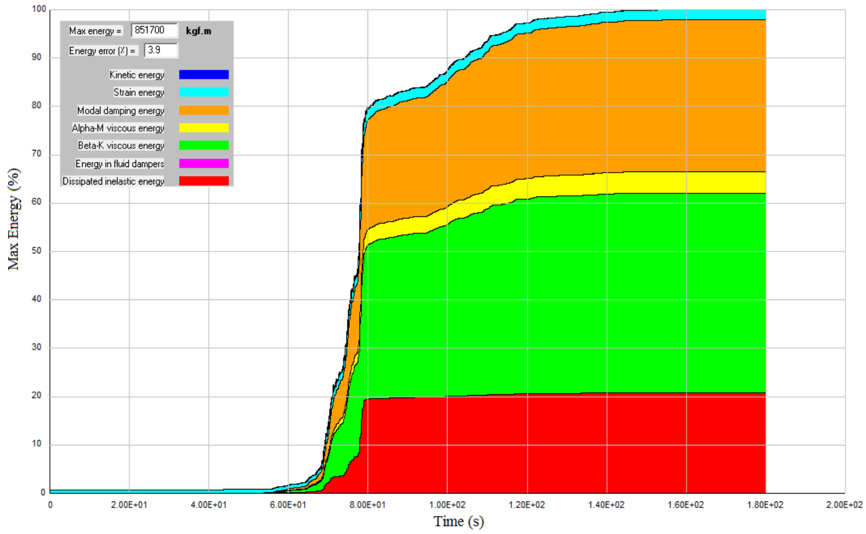

Figure 25. Energy plots for the 8-story structure with core shear wall under the chi chi record.

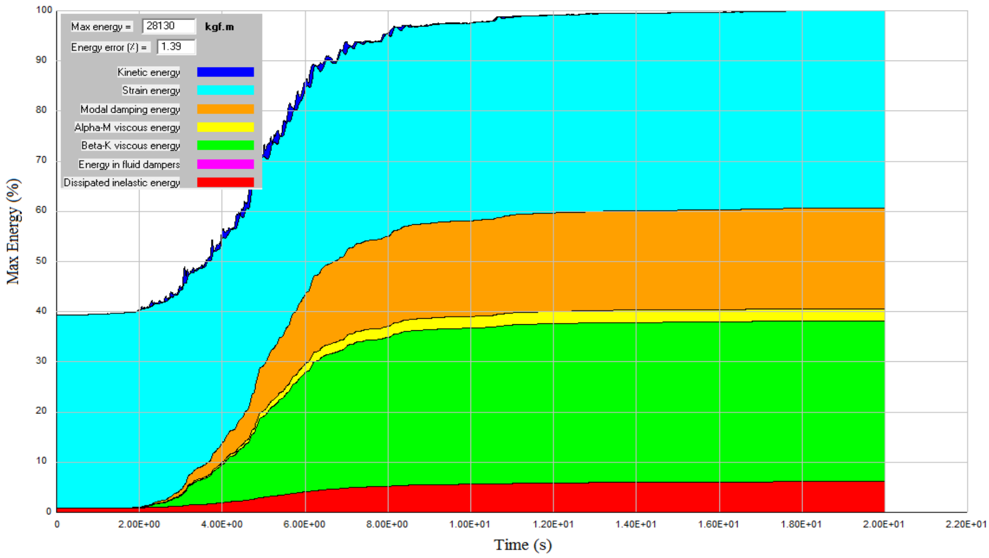

Figure 26. Energy plots for the 8-story structure with core shear wall under the Northridge record.

the energy graphs for a 8-story structure with core shear wall under the chi chi record, indicates that after 60 seconds the structure enters to the nonlinear phase, the minimum amount of the dissipated energy is obtained from the kinetic energy of masses and dissipated energy in fluid dampers and the maximum amount of the dissipated energy is corresponding to the viscose energy by βk dissipating. The amount of energy input to the structure is 851700 (kgf.m) and the energy error percentage for this earthquake is 3.39. In other hand the energy plots for the 8-story structure with core shear wall under the Northridge record, indicates that after 2 seconds, the structure enters to the nonlinear phase, the minimum amount of the dissipated energy is obtained from the kinetic energy of masses and the maximum amount of the dissipated energy is due to the reversible strain energy (hardening) in the elements and the viscose energy by βk dissipating. The amount of energy input to the structure is 28130 (kgf.m) and the energy error percentage for this earthquake is 1.39.

Conclusion

With the analyses of the above-mentioned structures, it can be seen that with the increasing in the magnitude of the selected earthquake, the performance level of the structures exceed the IO level and approximates the Ls level. From this result can be concluded that the concrete structures with the peripheral shear wall have a better performance level under the earthquakes with the greater magnitude. In addition, the energy input to the structure and the energy error percentage are increased by rising the magnitude (PGA) and duration of the selected earthquake.

References

Areias, P.M.A., Belytschko, T. (2005). Analysis of Three-Dimensional Crack Initiation and Propagation Using the Extended Finite Element Method. International Journal for Numerical Methods in Engineering, 63 (55), pp: 760-788.

Atluri, S.N., Shen, S. (2002). The Meshless Local Petrov–Galerkin (MLPG) Method. Tech Science Press, USA.

Udwadia, F.E., Trifunac, M.D. (1973). Ambient Vibration Test of Full Scale Structures. Proc. of the 5th World Conf. On Earthquake Engineering, Rome.

Fiuooz, A. (1369). Study on Dynamic characteristic of Concrete Hives by ambient Vibration Method. Master's Thesis, Shiraz University, Shiraz.

Trifunac, M.D. (1970). Wind and Microtremor Induced Vibration of a 22 Story Steel Frame Building. Earthquake Engineering Research Lab., Report EERL 70-01, California Institute of Technology, Pasadena California.

Sethian, J.A. (2006). Moving interfaces and boundaries: level set methods and fast marching methods. Available from: http://math.berkeley.edu/~sethian/Explanations/level_set_explain.html

Ali Hiuri, M.H, Sharifi, M.B. (1379). Water demand forecasting using artificial neural networks. Proceedings of the 5th International Conference on Civil Engineering, Ferdowsi University, Mashhad, Iran, May 21-19, 4: 1953-1953.

Citation: Ahmadi, A., Haghighatbin, F. (2018). Evaluation of the usage ratio graphs and energy dissipation in concrete structures with shear walls, under different earthquake records. Ukrainian Journal of Ecology, 8(3), 124–139.